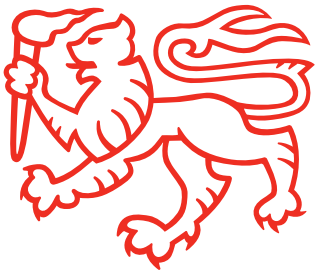

UNIVERSITY of TASMANIA

PART II LABORATORY WORK

KYA 211/212

Ultrasonic Ranging

Last compiled 2026-04-02

Safety

The experiment is set up on a moveable trolley. Care should be taken when moving this around the laboratory space. Before moving the trolley to different locations, check that the main power plug is out of the way.

Outline

Summary

In this experiment, we will be using ultrasonic sound waves to explore how the speed of sound is influenced by changing temperature and humidity conditions.

Experiment Objectives

- **Primary:** Explore the air temperature variability of the speed of sound by comparing results at two temperatures.
- **Secondary:** Observe and record the time taken for an ultrasonic signal to be transmitted and received and estimate the effects of humidity on the speed of sound in air.

Pre-lab Exercises

Pre-lab questions should be completed and submitted before you commence a new experiment. The information needed to complete the exercises is contained in the Background Theory Section, your course notes, or in the Appendices however, your own, independent research is highly encouraged. Make sure you include references where material has been sought elsewhere. This is not only “good form" but making notes of important information is essential if you then need to go back to that reference.

Task

1. Starting from equation 1, derive an expression for the speed of sound in an ideal gas that depends on the temperature of the gas. Why is pressure not important in determining the speed of sound?
2. Explain how humidity affects the speed of sound? Justify your argument with relevant equations and derivations. The paper from Bohn 1988 in the appendix will be helpful here.
3. How might reflections and environmental noise affect ultrasonic measurements? What methods can be used to mitigate these issues?
4. What is the effect of audio frequency on the speed of sound on Earth? Would this change on another planet like Mars, where the atmospheric composition is different? The article by Maurice et al. 2022 in the Appendices will be useful here. This work used data from the microphone on Perseverance’s SuperCam instrument. It was the first time in situ audio recordings of the Martian soundscape have been taken and analysed.

Background Theory

Ultrasonic ranging is a reliable and commonly used technique to measure the distance from a sensor to an object. It involves an ultrasonic transmitter sending out pulses of sound waves at a frequency above human hearing (above 20 kHz) which are picked up by a receiver after reflecting off the target as shown below in Fig. 1. Common applications

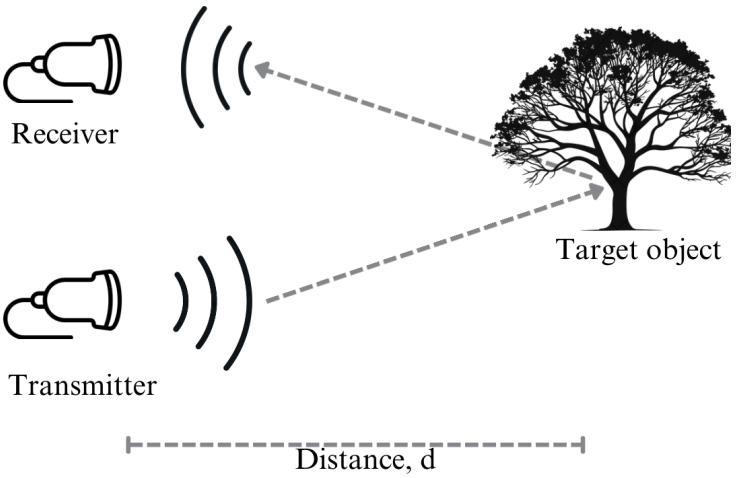

Figure 1: A simple schematic of ultrasonic ranging.

of ultrasonic ranging include surveying and mapping, parking assistance in vehicles, determining the fill level in a water tank, and medical imaging.

By measuring the time delay between transmitting and detecting these signals, and by knowing the speed of sound in the medium, the distance to an object can be calculated. In this experiment, we are instead going to use known distance measurements to explore how the speed of sound changes under different temperature and humidity conditions.

The speed of sound

Sound waves propagate as longitudinal waves, where the propagation speed is dependent on the properties of the medium through which they travel. For sound waves propagating through a fluid, the speed of sound is given by the Newton-Laplace equation

$$v = \sqrt{\frac{K_s}{\rho}} \tag{1}$$

Where K_s is the coefficient of stiffness or isentropic bulk modulus. Generally, $K_s = \rho \left(\frac{\partial P}{\partial \rho}\right)_s$ where the derivative is taken at constant entropy, s. In the case of sound propagation through an ideal gas, the bulk modulus is simply γP where γ is the dimensionless heat capacity ratio or adiabatic index. It describes the ratio of specific heat of a gas at constant pressure to that at constant volume, $\gamma = C_P/C_V$. The heat capacity ratio depends on the number of degrees of freedom of the molecules that comprise the gas. This, in turn, depends on the complexity of the molecules. Generally, $\gamma = 1.67$ for monatomic molecules, $\gamma = 1.40$ for diatomic molecules, and $\gamma = 1.33$ for triatomic molecules.

Apparatus

The ultrasonic ranging experiment is contained on a trolley. The setup allows you to send a signal, rebound it off a target (like a window) and receive it. As the trolley is movable, you are also able to change the distance to that target.

On the trolley, you have the following items. A labeled diagram of the key components is also shown in Fig. 2:

- An ultrasonic transmitter and receiver pair
- An Arduino and signal generator to control the transmitter output.
- Oscilloscope
- Amplifier
- Power supply
- Temperature and humidity sensor
- A tape measure

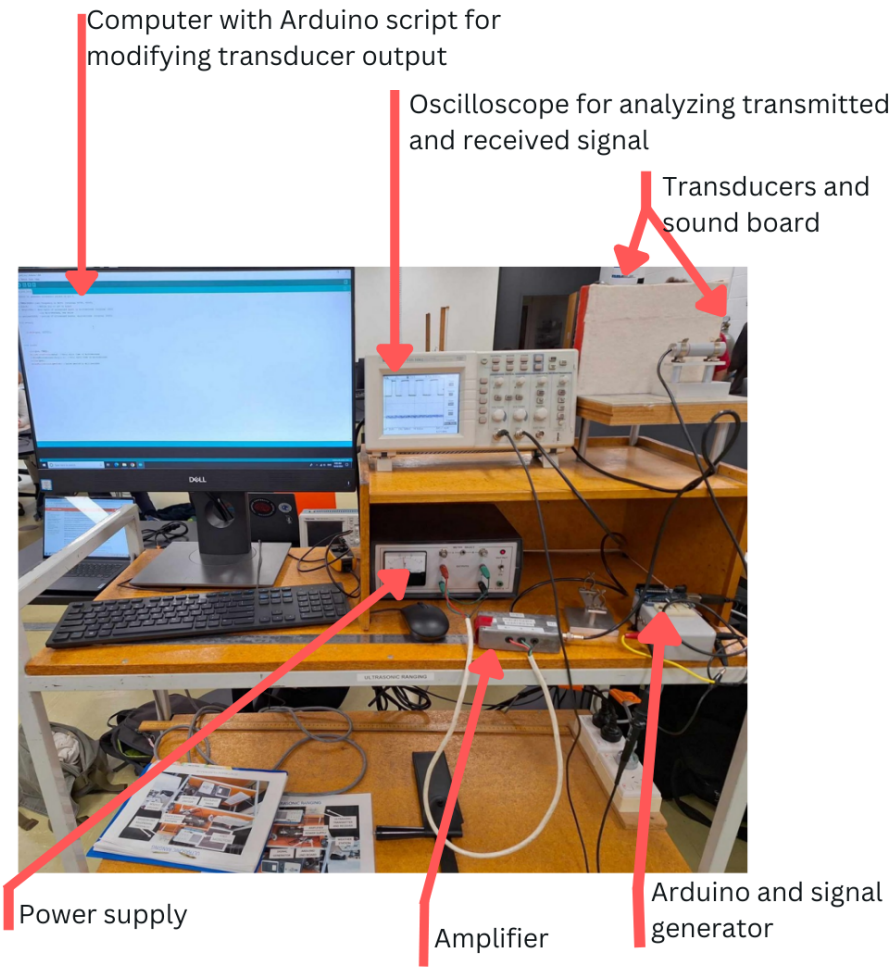

Figure 2: The components needed for the Ultrasonic Ranging lab.

Controlling the signal output

On the trolley, you have a pair of transducers (a receiver and transmitter) where the properties of the transmitted signal are controlled by an Arduino connected to a signal generator. Anything that is picked up by the receiver is sent through an amplifier and then into the oscilloscope for analysis. You will also be able to analyse the transmitted signal on the other oscilloscope channel.

The transducers are designed to operate at about 40 kHz. It is advantageous, however, to "fine tune" your pair so that they are operating at peak efficiency. You should do this in the preliminary steps of carrying out your experiment.

On the accompanying computer, you will have a file called `tone_pin8.ino` which should be located at `C:\Users\Public\PublicDocuments\Ultrasonic\tone_pin8.ino`. This allows you to change the properties of the signal being transmitted.

This file has comments next to the commands which should explain what each one does. Within the script, the following variables are defined:

- `FREQ` allows you to set the frequency of the ultrasound emitted. Edit the value to about 40 kHz and fine tune as you see fit.
- `duty` or duty cycle, sets how long each ultrasonic pulse lasts. In microseconds.
- `period` sets the time between the pulses. Also in microseconds.

The "setup" section configures the hardware on the board, the "loop" section has commands which are repeated endlessly. You should not need to edit these sections.

Save the file (shortcut; `Ctrl+S`). The new parameters are loaded on the board by uploading the sketch file to the Arduino, (shortcut; `Ctrl+U`). The Arduino then feeds this information to the signal generator.

Procedure

With the apparatus described and the relevant physics discussed, it is now time to design and execute the experiment that achieves the Experiment Objectives.

Task

Design an experiment plan that will allow you to determine the effects of humidity and temperature on the speed of sound in air. In planning, it will help to consider the following questions:

1. How will you validate the operation of the equipment? That is, how will you know the receiver is indeed picking up the signal from the transmitter? You should design some simple tests to make sure your equipment is working properly.
2. What is the principle data you need to take? How will the equipment help you do this (think about the functions on the oscilloscope)?
3. What sort of meteorological observations do you need to make and when might you make them?
4. What sort of errors exists and how they might be mitigated? Remember to note estimates of distance and time measurement errors, as well as temperature and humidity error. These will all contribute to an error in velocity.

5. How many samples should each dataset contain?

Discuss this with your demonstrators before you get started and record your experiment plan in your logbooks.

While carrying out your experiment, remember to include the following in your logbooks

1. Labelled diagrams of your setup.
2. Details of your process including processes which didn't end up working out.
3. Assumed values.
4. Sources of error.
5. Sanity checks to validate your initial observations and any preliminary results. In other words, how do you know you're on the right track before you get to your final results?

Calculations and Discussion

Having carried out your experiment, you can now consider analysing your ultrasonic signal transit time measurements.

Task

1. Make a plot of the transit time versus distance. Use the plot or software to calculate the speed of sound for each set of your measurements.
2. In the pre-lab section, you derived an equation for the speed of sound that depends on temperature and estimated the effects of humidity. How do the trends in your data compare to this? How do your trends compare to those discussed in Bohn 1988?
3. From your results, what are the relative magnitudes of the effects of temperature and humidity?

As you process your results, remember to **propagate your errors and display error bars on key plots.**

References

Bohn, Dennis A (1988). "'Environmental effects on the speed of sound'". In: *'Journal of Audio Engineering'*.

Maurice, S. et al. (2022). "In situ recording of Mars soundscape". In: *Nature* 605.7911, pp. 653–658. DOI: 10.1038/s41586-022-04679-0.

1 Appendices

Article

In situ recording of Mars soundscape

https://doi.org/10.1038/s41586-022-04679-0

Received: 7 December 2021

Accepted: 23 March 2022

Published online: 1 April 2022

Open access

Check for updates

S. Maurice[1]✉, B. Chide[2]✉, N. Murdoch[3], R. D. Lorenz[4], D. Mimoun[3], R. C. Wiens[2,5], A. Stott[3], X. Jacob[6], T. Bertrand[7], F. Montmessin[8], N. L. Lanza[2], C. Alvarez-Llamas[9], S. M. Angel[10], M. Aung[11], J. Balaram[11], O. Beyssac[12], A. Cousin[1], G. Delory[13], O. Forni[1], T. Fouchet[7], O. Gasnault[1], H. Grip[11], M. Hecht[14], J. Hoffman[15], J. Laserna[9], J. Lasue[1], J. Maki[11], J. McClean[14], P.-Y. Meslin[1], S. Le Mouélic[16], A. Munguira[17], C. E. Newman[18], J. A. Rodríguez Manfredi[19], J. Moros[9], A. Ollila[2], P. Pilleri[1], S. Schröder[20], M. de la Torre Juárez[11], T. Tzanetos[11], K. M. Stack[11], K. Farley[11], K. Williford[11,21] & the SuperCam team*

Before the Perseverance rover landing, the acoustic environment of Mars was unknown. Models predicted that: (1) atmospheric turbulence changes at centimetre scales or smaller at the point where molecular viscosity converts kinetic energy into heat[1], (2) the speed of sound varies at the surface with frequency[2,3] and (3) high-frequency waves are strongly attenuated with distance in CO_2 (refs. [2–4]). However, theoretical models were uncertain because of a lack of experimental data at low pressure and the difficulty to characterize turbulence or attenuation in a closed environment. Here, using Perseverance microphone recordings, we present the first characterization of the acoustic environment on Mars and pressure fluctuations in the audible range and beyond, from 20 Hz to 50 kHz. We find that atmospheric sounds extend measurements of pressure variations down to 1,000 times smaller scales than ever observed before, showing a dissipative regime extending over five orders of magnitude in energy. Using point sources of sound (Ingenuity rotorcraft, laser-induced sparks), we highlight two distinct values for the speed of sound that are about 10 m s^{-1} apart below and above 240 Hz, a unique characteristic of low-pressure CO_2-dominated atmosphere. We also provide the acoustic attenuation with distance above 2 kHz, allowing us to explain the large contribution of the CO_2 vibrational relaxation in the audible range. These results establish a ground truth for the modelling of acoustic processes, which is critical for studies in atmospheres such as those of Mars and Venus.

Before the landing of Perseverance (18 February 2021), no pressure fluctuations had ever been monitored on Mars at a frequency >20 Hz, namely, in the acoustic domain. The recording of sounds offers the unique opportunity to study the atmosphere as the main natural source of sound and as the propagation medium for acoustic waves. From the knowledge of Mars atmospheric pressure (about 0.6 kPa) and the physical properties of CO_2, one can predict (see Methods) that: the acoustic impedance results in approximately 20 dB weaker sounds on Mars than on Earth if produced by the same source, the speed of sound should be around 240 m s^{-1} near the surface and acoustic waves are heavily damped in CO_2 at these atmospheric pressures and temperatures. A few studies[2,3] proposed very detailed models of acoustic propagation on Mars but with large discrepancies between their results because of a lack of experimental data at low pressure and appropriate temperatures, and the difficulty of characterizing attenuation in a closed environment. Acoustic data are also sensitive to wind speed and direction and, to a lesser extent, other environmental parameters[5,6]. As such, owing to the high sampling frequency of microphones (up to 100 kHz), the acoustic data allow us to explore the atmospheric behaviour on a microscale that has never been accessible before on Mars.

The SuperCam instrument suite[7,8] on Perseverance carries an electret microphone, similar to that carried by the Mars Polar Lander[9], lost during atmospheric entry, and the Phoenix spacecraft[10], on which technical issues prevented the device from being operated. SuperCam's microphone is able to record air pressure fluctuations from 20 Hz to 12.5 kHz or 50 kHz, at sampling rates of 25 kHz or 100 kHz, respectively. After landing (Martian

[1]Institut de Recherche en Astrophysique et Planétologie, Université de Toulouse 3 Paul Sabatier, CNRS, CNES, Toulouse, France. [2]Space and Planetary Exploration Team, Los Alamos National Laboratory, Los Alamos, NM, USA. [3]Institut Supérieur de l'Aéronautique et de l'Espace (ISAE-SUPAERO), Université de Toulouse, Toulouse, France. [4]Space Exploration Sector, Johns Hopkins Applied Physics Laboratory, Laurel, MD, USA. [5]Present address: Department of Earth, Atmospheric, and Planetary Sciences, Purdue University, West Lafayette, IN, USA. [6]Institut de Mécanique des Fluides, Université de Toulouse 3 Paul Sabatier, INP, CNRS, Toulouse, France. [7]Laboratoire d'Etudes Spatiales et d'Instrumentation en Astrophysique, Observatoire de Paris, CNRS, Sorbonne Université, Université Paris Diderot, Meudon, France. [8]Laboratoire Atmosphères, Milieux, Observations Spatiales, CNRS, Université Saint-Quentin-en-Yvelines, Sorbonne Université, Guyancourt, France. [9]Universidad de Málaga, Málaga, Spain. [10]Department of Chemistry and Biochemistry, University of South Carolina, Columbia, SC, USA. [11]Jet Propulsion Laboratory, California Institute of Technology, Pasadena, CA, USA. [12]Institut de Minéralogie, de Physique des Matériaux et de Cosmochimie, CNRS, Sorbonne Université, MNHN, Paris, France. [13]Heliospace Corporation, Berkeley, CA, USA. [14]Haystack Observatory, Massachusetts Institute of Technology, Westford, MA, USA. [15]Department of Aeronautics and Astronautics, Massachusetts Institute of Technology, Cambridge, MA, USA. [16]Laboratoire de Planétologie et Géosciences, CNRS, Nantes Université, Université Angers, Nantes, France. [17]Escuela de Ingeniería de Bilbao, Universidad del País Vasco UPV/EHU, Bilbao, Spain. [18]Aeolis Corporation, Sierra Madre, CA, USA. [19]Centro de Astrobiología (INTA-CSIC), Madrid, Spain. [20]Deutsches Zentrum für Luft- und Raumfahrt (DLR), Institute of Optical Sensor Systems, Berlin, Germany. [21]Blue Marble Space Institute of Science, Seattle, WA, USA. *A list of authors and their affiliations appears at the end of the paper. ✉e-mail: sylvestre.maurice@irap.omp.eu; bchide@lanl.gov

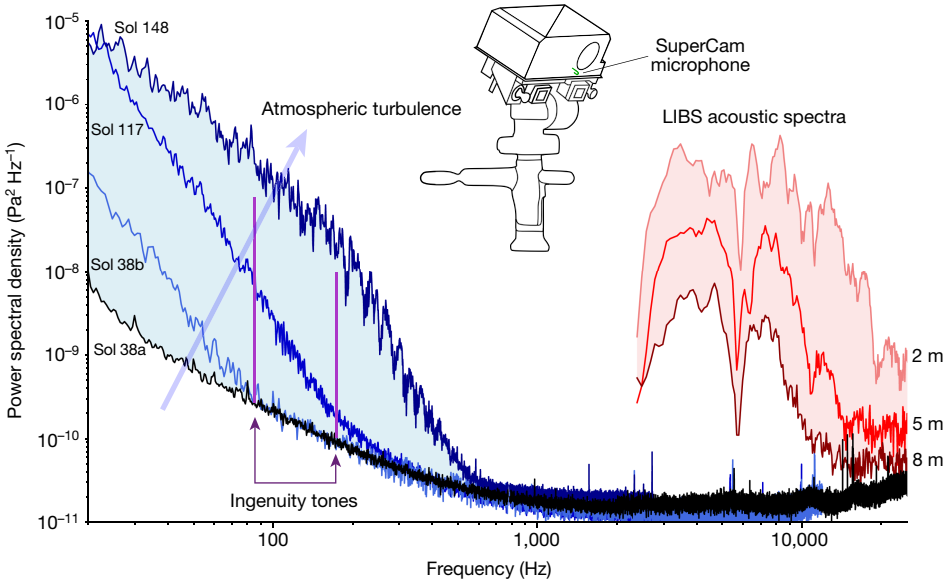

Fig. 1 | Variety of sounds recorded by SuperCam. Atmospheric spectra spread over the light blue area; turbulence increases in the direction of the arrow. LIBS acoustic spectra spread over the light red area. Ingenuity tones are recorded at 84 Hz and 168 Hz (purple). The black spectrum is the quietest recording so far below 1 kHz. SuperCam's microphone is located on the rover mast (green).

solar day 'Sol' 0; one Sol = 88,775 s), the microphone was turned on for the first time on Sol 1 while the mast was still stowed. Since deployment on Sol 2, the microphone is approximately 2.1 m above the ground; it has performed nominally up to the time of writing. SuperCam also consists of a laser-induced breakdown spectroscopy (LIBS) capability to analyse the chemistry of Mars at stand-off distances from 1.5 to 7 m (refs. [7,8]). When the laser pulse interacts with the target, a luminous plasma emits characteristic optical emission lines of the elements present in the target[11]. Plasma expansion generates a shock wave that decouples from the plasma within the first microsecond after laser interaction[12] and results in a clearly detectable acoustic signal[13,14]. Moreover, Perseverance carries a second microphone as part of the Entry, Descent, and Landing Camera (EDLCAM[15]), which has a frequency response from 20 Hz to 20 kHz at a sampling rate of 48 kHz. The EDL microphone is mounted on the port side of the rover, 1 m above the ground. It was activated on Sol 2.

Figure 1 provides an overview of sounds acquired by SuperCam's microphone (see Methods). Sol 38a is the quietest recording in our dataset. Later on that same day (Sol 38b), the power spectral density (PSD) increases above the quiet state at frequencies below 100 Hz. On Sol 117, we associate this increase of power to an increase in the turbulent activity, which extends up to 300 Hz; this is the situation we observe most often. The recording of Sol 148 is the most active one shown, with the same shape starting towards higher frequencies but with a slope break near 200 Hz; turbulence is detected up to 600 Hz. All non-saturated atmospheric recordings from Sol 0 to Sol 216 fit between the boundaries given by the Sol 38a and Sol 148 spectra. The laser-excited plasma generates a short, roughly 300-µs acoustic pulse (see Methods), with 95% of its energy between 3 and 15 kHz. Various spectral notches are caused by acoustic interferences owing to echoes from the base of the microphone itself (6 kHz and 12 kHz) or from nearby rocks. The total intensity varies as a function of target distance, as shown for recordings at 2 m, 5 m and 8 m. During laser-induced spark recording sessions, the atmospheric signal below 1 kHz is masked by electromagnetic interference[8]. The Ingenuity rotorcraft tones (see Methods) are also shown.

Atmospheric turbulence

The Martian planetary boundary layer (PBL) is the part of the atmosphere in contact with the surface[16], extending to several km. It is prone to convective turbulence and vertical mixing during daytime, owing to the thin atmosphere and low surface thermal inertia that induce strong and unstable near-surface temperature gradients[17–19]. This turbulence translates into high-frequency variations in atmospheric pressure, wind speed and temperature that can be measured by in situ instruments. Conversely, during night-time, the strong radiative cooling of the atmosphere induces highly stable conditions, which efficiently inhibit most convection and turbulence[16]. Analysing the PBL at the surface is therefore important to understand how the Martian atmosphere transports and mixes heat, momentum, aerosols and chemical species[20]. The Mars Environmental Dynamics Analyzer (MEDA[21]) instrument on Perseverance and the meteorological suites of previously landed missions[20,22] typically measure pressure, temperature and wind fluctuations with sampling frequencies of 0.1 Hz to 10 Hz. These instruments study the turbulence variability[23,24] and the Martian turbulent energy cascade[1,17,25].

Specifically, we report here the observation of the dissipative turbulence regime in the PBL, in which the InSight mission could see a hint of a regime change at the limits of the instrument capability[1]. This regime, in which molecular viscosity dissipates the turbulent kinetic energy into heat, is now fully characterized by a rapid decrease of the power spectrum with increasing frequency (Fig. 1, 2b) over roughly five orders of magnitude. The scale at which the viscous dissipation becomes notable is characterized by the Kolmogorov length scale[26], $\eta = (\nu^3/\varepsilon)^{0.25}$, in which ν is the kinematic viscosity and ε is the turbulence energy dissipation rate per unit mass, typically around 0.001 $m^2\,s^{-1}$ and 0.005 $m^2\,s^{-1}$ on Mars, respectively[17]. Thus η is about 0.02 m and the timescale of these small eddies, $t_\eta = (\nu/\varepsilon)^{0.5}$, is about 0.45 s. Hence the dissipation regime should be observable at frequencies above 2 Hz on Mars, at centimetre or smaller scales only (on Earth, this transition occurs at millimetre scales or smaller[17]). This theoretical prediction is confirmed by the acoustic data; the threshold moves with frequency, depending on the dissipation rate[25,27]. The balance between energy production and molecular dissipation controls the total amount of turbulent kinetic energy in the boundary layer and, as such, the dissipation mechanism is intrinsically linked to the PBL dynamics; a larger dissipation leads to a faster turbulence decay, in turn suppressing small-scale wind gustiness, and vice versa.

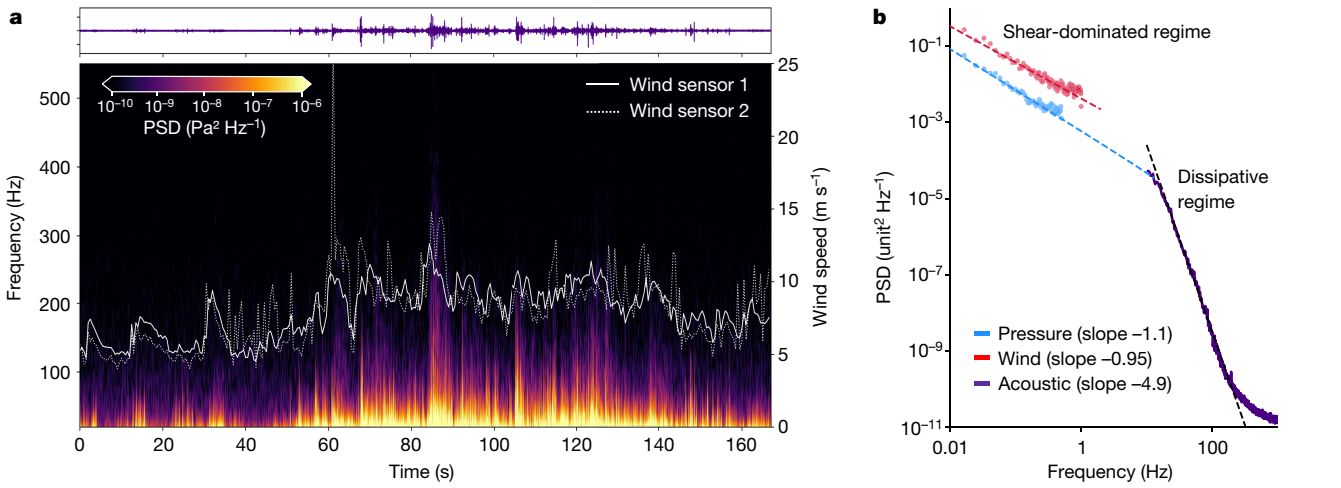

Fig. 2 | Sound recordings and correlation with atmospheric data. Recording of Sol 38b. **a**, On top, the *y* axis of the time series ranges from −0.2 to 0.2 Pa. The spectrogram (bottom) shows bursts that extend to 300 Hz. Overlaid, with the *y* axis on the right, are wind speeds from MEDA booms. **b**, The PSD calculated for SuperCam's microphone (in $Pa^2\,Hz^{-1}$ for 167 s) and for MEDA pressure (in $Pa^2\,Hz^{-1}$ for 51 min around the microphone acquisition time) and MEDA wind data (in $(m\,s^{-1})^2\,Hz^{-1}$). The wind PSD is artificially offset by 10^{-2} in the *y* axis.

The microphone records rapid deviations from ambient pressure (>20 Hz) that are correlated to variations in the wind flow, as shown by Fig. 2a, in which a spectrogram of Sol 38b microphone data (see Methods) is overlaid with the wind speed as measured by the MEDA (see Methods). As expected[6,13], there is a clear correlation between the intensity of acoustic data and the wind speed. This can be owing to the flow-induced turbulence from the rover/mast itself but also to the direct sensing of the incoming flow fluctuations, seen to be the dominant factor for outdoor microphones in other studies[6]. Moreover, the daytime local turbulence is known to increase for larger ambient wind speeds[24]. The high microphone sampling rate provides an opportunity to observe very intense but short wind gusts, on a timescale of 10 s. In Fig. 2b, the same acoustic data are plotted in the frequency domain and combined with low-frequency measurements of pressure and wind from the MEDA, for a 51-min time period of continuous data around the microphone acquisition. The large difference in slope between the MEDA and microphone data is indicative of regime change. The transition from the probable shear-dominated regime[28] to the dissipation regime occurs in this case between 1 and 20 Hz.

Speed of sound on Mars

In a cold CO_2 atmosphere, the speed of sound is expected to be lower than on Earth. Furthermore, owing to the low pressure and the physical properties of CO_2, we also expect a dispersion of this speed with frequency[2,3]. On Earth, the adiabatic ratio γ is constant up to a few MHz at ambient pressure[29] and sound speed does not vary with frequency near the surface. At low pressure on Mars, still within the framework of small Knudsen numbers[30] (10^{-6} at 100 Hz to 2.10^{-4} at 20 kHz), the continuum theory still holds, but energy exchanges at molecular scales are modified. Part of the energy associated with the translational motions of molecules, which constitute the acoustic waves, is spent on the excitation of inner degrees of freedom (vibrational modes and rotational motions). The relaxation of the rotational motion is almost instantaneous, whereas relaxation of the vibrational modes occurs over a much longer timescale, a property of small and rigid polyatomic molecules such as CO_2. If the frequency f is smaller than $f_R = 1/\tau_R$, in which τ_R is the relaxation time, all modes are equally excited and then relaxed. The seven degrees of freedom that result from three translational modes, two rotational modes and one doubly-degenerate vibrational mode (v_2, bending) lead to an adiabatic index $\gamma_0 = 9/7 = 1.2857$. Conversely, if $f > f_R$, there is no time to relax the vibrational mode; in that case, there are only five active degrees of freedom and $\gamma_\infty = 7/5 = 1.4$. In CO_2 at Earth-ambient pressure, f_R is about 40 kHz (ref. [31]). This frequency depends on the rate at which molecules can collide, hence f_R is proportional to the pressure. As a result, at 0.6 kPa, the relaxation frequency is about 240 Hz on Mars.

The recording of pulsed waves generated in LIBS mode provides a unique opportunity to measure directly and repetitively the local speed of sound for acoustic waves above 2 kHz, that is, for $f > f_R$ (see Methods). From the daytime measurements, sound speeds between 246 m s^{-1} and 257 m s^{-1} are obtained (Fig. 3a), with maximum values between 11:00 to 14:00 Local True Solar Time (LTST) and minimum values around 18:00. The 1σ-dispersion of the sound speed during the approximately 20 min of a target analysis with LIBS is at its maximum at noon (1.5%) and is reduced to 0.5% at 18:00, which highlights the vanishing of the atmospheric turbulence at dusk. These measurements are compared with temperature-derived speeds of sound obtained from: (1) the MEDA temperature datasets at the surface, at the heights of 0.85 m and 1.45 m, and (2) the temperature at the surface and at a height of 2 m given by the Mars Climate Database (MCD[32]) (see Methods), using $\gamma_\infty = 1.4$ (because $f > f_R$). The agreement between the MEDA and MCD predictions is excellent. SuperCam sound speeds are comparable with temperature-derived values at the height of the MEDA's 0.85-m temperature sensor or higher. This is consistent with the fact that the speed is integrated between a height of 2.1 m and the surface, possibly biased towards the surface when the temperature gradient is larger.

Ingenuity's blade passage frequency (BPF)[33] is close to a harmonic source centred around 84 Hz, and – in that case – for $f < f_R$ (see Methods). This signal recorded by SuperCam's microphone is modulated by the variations of the distance range between the microphone and the helicopter. An emitted frequency at 84.43 Hz and a speed of sound $c = 237.7 \pm 3$ m s^{-1} are estimated on the basis of a fit of the Doppler effect for Ingenuity's fourth flight (see Methods). Accounting for the presence of a wind of about 2.5 m s^{-1} along the microphone-to-helicopter line of sight towards the helicopter (MEDA data), the true sound speed is about 240 m s^{-1} at this frequency. At the time of the flight, the atmospheric temperatures ranged between 232 K and 240 K at a height of 1.45 m. Using $\gamma_0 = 1.2857$ (the BPF is below f_R), the temperature-derived speed of sound ranges from 238.8 m s^{-1} to 242.9 m s^{-1}, which is consistent with the speed directly derived from Ingenuity's flight plus wind (Fig. 3b). As a summary, SuperCam's microphone highlights a sound speed dispersion of about 10 m s^{-1} in the audible range at the surface of Mars.

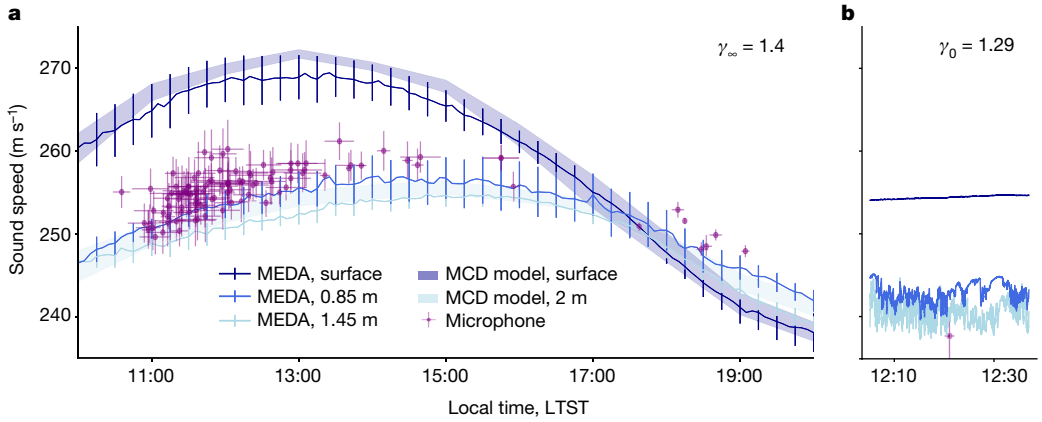

Fig. 3 | Sound speed variations. a, Sound speeds as a function of local time from LIBS time-of-flight data in purple. Other sound speeds are calculated at the three heights from the MEDA temperatures and at the surface and at 2-m altitude from MCD simulations; for these conversions, the adiabatic index above f_R is used. Error bars for microphone data: standard deviation of the sound speeds during each laser burst (vertical); total duration of the burst (horizontal). Error bars for the MEDA data: standard deviation of 1-h bins between Sols 37 and 216. **b**, Sound speeds are calculated at three heights from the MEDA temperatures during Ingenuity's fourth flight; the adiabatic index below f_R is used. The sound speed estimated from the Ingenuity Doppler effect is in purple. Error bars: 95% confidence interval of the Doppler shift fit.

Sound attenuation

The most remarkable property of sound propagation on Mars is the magnitude of the attenuation at all frequencies, especially above 1 kHz. The decrease of the LIBS acoustic signal with distance is an opportunity to verify the theory in situ and to test two different attenuation models[3,4] that suffer from a lack of field data under Mars conditions.

As the spherical LIBS acoustic wave propagates, sound pressure decreases as $1/r$, in which r is the distance between the target and the microphone. This decrease is scaled by a factor $r^{-0.698}$ to account for the variation of laser irradiance[8], multiplied by $e^{-\alpha r}$, in which $\alpha = \alpha(f)$ is the atmospheric attenuation coefficient as a function of frequency. The frequency spectrum of the LIBS acoustic signal is divided into three bands, which account for the three main lobes observed in Fig. 1: from 3 kHz to 6 kHz, from 6 kHz to 11 kHz and from 11 kHz to 15 kHz. The evolution of the sound amplitude with distance for the second frequency band is shown in Fig. 4a. Over the three bands, we find $\alpha = 0.21 \pm 0.04$ m^{-1} (95% confidence interval of the fit), $\alpha = 0.34 \pm 0.05$ m^{-1} and $\alpha = 0.43 \pm 0.05$ m^{-1} respectively. As expected, high-pitched sounds are strongly attenuated. Compared with a signal emitted at 1 m, attenuation of an 8-kHz wave ranges from −9 dB at 2 m to −40 dB at 8 m. At 5 m, the atmospheric absorption takes precedence over the geometrical attenuation. On Earth, for which $\alpha = 0.01$ m^{-1} for the same frequency[34], the attenuation ranges from −6 dB at 2 m to −20 dB at 8 m, and is almost exclusively resulting from the wavefront spreading. To reach an attenuation of −40 dB on Earth, the source would need to be at 65 m.

Such attenuation coefficients are compared with theoretical[3] and semi-empirical[4] attenuation models in Fig. 4b. In situ data tend towards the behaviour described by Bass and Chambers[3], with a plateau at frequencies <6 kHz and then an increase for higher frequencies. Conversely, the data do not show an attenuation gap as suggested by the model of Williams[4]. This result confirms the large contribution of CO_2 vibrational relaxation in this frequency range, the same process that explains the two values for the speed of sound (above). However, the attenuation coefficient for the 2–6-kHz band is still higher than that predicted by Bass and Chambers[3]. It may highlight a different relaxation

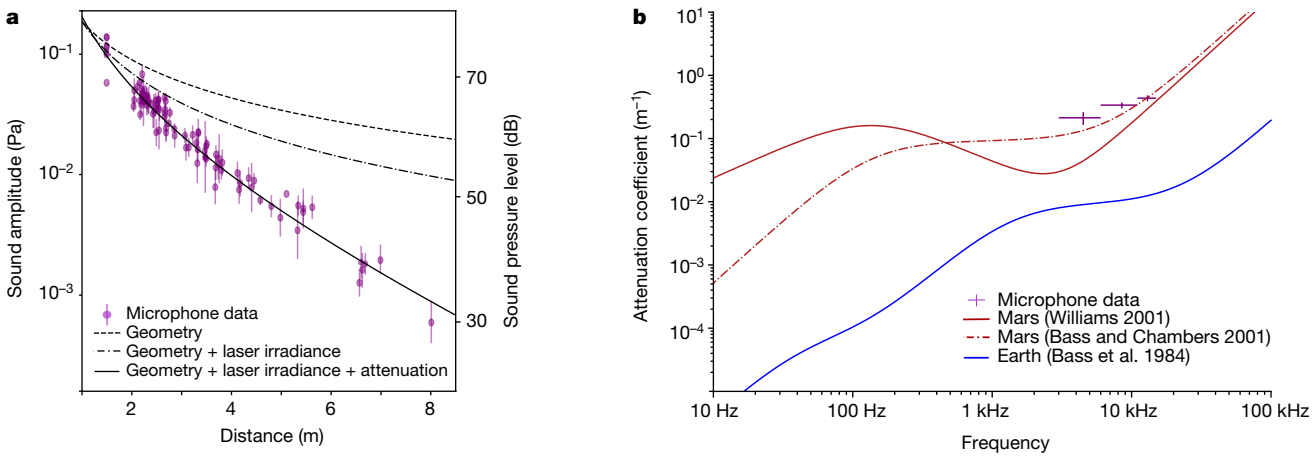

Fig. 4 | Sound attenuation with distance. a, Sound amplitude as a function of target distance r from LIBS acoustic data between 6 kHz and 11 kHz. The second vertical axis on the right is for sound pressure level in dB. Signal intensities are in dB relative to 20 µPa. Error bars: standard deviation of the acoustic amplitudes during each laser burst. **b**, Comparison of the attenuation models for Mars[3,4] (computed at 240 K and 740 Pa) and Earth[34] (293 K and 30% relative humidity). The experimental points correspond to this study. Error bars: 95% confidence interval of the fit performed in Fig. 4a (vertical) and width of each frequency range (horizontal).

strength than the one forecasted by the model (see Methods). However, these measurements do not reach frequencies low enough to constrain the large discrepancies observed between models below 1 kHz.

Mars soundscape

Sound is a new, rich source of information on Mars. Thanks to sensors measuring only a few millimetres in diameter, turbulence-induced noise and artificial sources have been recorded. Acoustic waves are governed by the macroscopic thermodynamic properties of fluids (molar mass, heat capacity and temperature, or – alternatively – compressibility and density). However, given the small displacements and timescales that come into play, we confirm that energy exchanges at the molecular scale also need to be considered to accurately model the sound propagation parameter variations (speed, attenuation) with frequency. More sound speed measurements at different local times and seasons will allow the study of atmospheric fluctuations at a scale of a few metres on Mars[35–37]. The first in situ retrieval of the acoustic attenuation coefficient already provides new constraints on theoretical models, which are key parameters for geophysical studies in CO_2-dominated atmospheres[38,39]. Wind and turbulence, driven by heat fluxes, are natural sources of pressure fluctuations on Mars. We show that acoustic data yield new insights into the boundary layer turbulence with 10 to 1,000 times higher temporal resolution than before, highlighting for the first time the dissipative regime and a transition to this regime above a few Hz. Characterizing this regime in more detail, and the associated transition, is necessary to settle the assumptions used in the numerical modelling of the PBL (including large-eddy simulations), telling us what the fraction of missing energy is in the unresolved scales of the models[40,41]. In the future, this will lead to a measurement of the dissipation rate, related to the diffusion of heat in the atmosphere, which is not well known for Mars at present[17,42]. Finally, beyond the rumble of the wind, the acoustic signatures of our robotic presence on Mars are rich in information on the health of the rover subsystems.

Online content

Any methods, additional references, Nature Research reporting summaries, source data, extended data, supplementary information, acknowledgements, peer review information; details of author contributions and competing interests; and statements of data and code availability are available at https://doi.org/10.1038/s41586-022-04679-0.

1. Banfield, D. et al. The atmosphere of Mars as observed by InSight. *Nat. Geosci.* **13**, 190–198 (2020).
2. Petculescu, A. & Lueptow, R. M. Atmospheric acoustics of Titan, Mars, Venus, and Earth. *Icarus* **186**, 413–419 (2007).
3. Bass, H. E. & Chambers, J. P. Absorption of sound in the Martian atmosphere. *J. Acoust. Soc. Am.* **109**, 3069–3071 (2001).
4. Williams, J.-P. Acoustic environment of the Martian surface. *J. Geophys. Res.* **106**, 5033–5041 (2001).
5. Chide, B. et al. Experimental wind characterization with the SuperCam microphone under a simulated martian atmosphere. *Icarus* **354**, 114060 (2021).
6. Morgan, S. & Raspet, R. Investigation of the mechanisms of low-frequency wind noise generation outdoors. *J. Acoust. Soc. Am.* **92**, 1180–1183 (1992).
7. Wiens, R. C. et al. The SuperCam instrument suite on the NASA Mars 2020 rover: body unit and combined system tests. *Space Sci. Rev.* **217**, 4 (2021).
8. Maurice, S. et al. The SuperCam instrument suite on the Mars 2020 rover: science objectives and Mast-Unit description. *Space Sci. Rev.* **217**, 47 (2021).
9. Delory, G. T., Luhmann, J., Friedman, L. & Betts, B. Development of the first audio microphone for use on the surface of Mars. *J. Acoust. Soc. Am.* **121**, 3116–3116 (2007).
10. NASA. Mars Descent Imager (MARDI); www.nasa.gov/mission_pages/phoenix/spacecraft/mardi.html.
11. Miziolek, A. W., Palleschi, V. & Schechter, I. (eds) *Laser-Induced Breakdown Spectroscopy* (Cambridge Univ. Press, 2006).
12. Seel, F. *Laboratory Studies on Laser-Induced Shock Waves for LIBS Measurements on Mars*. Master's Thesis, Technische Universität Berlin (2021).
13. Chide, B. et al. Recording laser-induced sparks on Mars with the SuperCam microphone. *Spectrochim. Acta B At. Spectrosc.* **174**, 106000 (2020).
14. Murdoch, N. et al. Laser-induced breakdown spectroscopy acoustic testing of the Mars 2020 microphone. *Planet. Space Sci.* **165**, 260–271 (2019).
15. Maki, J. N. et al. The Mars 2020 engineering cameras and microphone on the Perseverance rover: a next-generation imaging system for Mars exploration. *Space Sci. Rev.* **216**, 137 (2020).
16. Savijarvi, H. A model study of the PBL structure on Mars and the Earth. *Contrib. Atmos. Phys.* **64**, 219–229 (1991).
17. Petrosyan, A. et al. The Martian atmospheric boundary layer. *Rev. Geophys.* **49**, RG3005 (2011).
18. Tillman, J. E., Landberg, L. & Larsen, S. E. The boundary layer of Mars: fluxes, stability, turbulent spectra, and growth of the mixed layer. *J. Atmos. Sci.* **51**, 1709–1727 (1994).
19. Larsen, S. E. et al. Aspects of the atmospheric surface layers on Mars and Earth. *Boundary Layer Meteorol.* **105**, 451–470 (2002).
20. Martínez, G. M. et al. The modern near-surface Martian climate: a review of in-situ meteorological data from Viking to Curiosity. *Space Sci. Rev.* **212**, 295–338 (2017).
21. Rodriguez-Manfredi, J. A. et al. The Mars Environmental Dynamics Analyzer, MEDA. A suite of environmental sensors for the Mars 2020 mission. *Space Sci. Rev.* **217**, 48 (2021).
22. Banfield, D. et al. InSight Auxiliary Payload Sensor Suite (APSS). *Space Sci. Rev.* **215**, 4 (2019).
23. Ullán, A. et al. Analysis of wind-induced dynamic pressure fluctuations during one and a half Martian years at Gale Crater. *Icarus* **288**, 78–87 (2017).
24. Chatain, A., Spiga, A., Banfield, D., Forget, F. & Murdoch, N. Seasonal variability of the daytime and nighttime atmospheric turbulence experienced by InSight on Mars. *Geophys. Res. Lett.* **48**, e2021GL095453 (2021).
25. Temel, O. et al. Large eddy simulations of the Martian convective boundary layer: Towards developing a new planetary boundary layer scheme. *Atmos. Res.* **250**, 105381 (2021).
26. Kolmogorov, A. N. The local structure of turbulence in incompressible viscous fluid for very large Reynolds numbers. *Cr. Acad. Sci. URSS* **30**, 301–305 (1941).
27. Chen, W., Lovejoy, S. & Muller, J.-P. Mars' atmosphere: the sister planet, our statistical twin. *J. Geophys. Res. Atmos.* **121**, 11,968–11,988 (2016).
28. Tchen, C. M. On the spectrum of energy in turbulent shear flow. *J. Res. Natl. Bur. Stand.* **50**, 51–62 (1953).
29. Bass, H. E., Hetzer, C. H. & Raspet, R. On the speed of sound in the atmosphere as a function of altitude and frequency. *J. Geophys. Res.* **112**, D15110 (2007).
30. Hanford, A. D. & Long, L. N. The direct simulation of acoustics on Earth, Mars, and Titan. *J. Acoust. Soc. Am.* **125**, 640–650 (2009).
31. Zhang, X., Wang, S. & Zhu, M. Locating the inflection point of frequency-dependent velocity dispersion by acoustic relaxation to identify gas mixtures. *Meas. Sci. Technol.* **31**, 115001 (2020).
32. Forget, F. et al. Improved general circulation models of the Martian atmosphere from the surface to above 80 km. *J. Geophys. Res.* **104**, 24155–24175 (1999).
33. Balaram, J., Aung, M. & Golombek, M. P. The Ingenuity Helicopter on the Perseverance Rover. *Space Sci. Rev.* **217**, 56 (2021).
34. Bass, H., Sutherland, L., Piercy, J. & Evans, L. in *Physical Acoustics: Principles and Methods* Vol. 17 (eds Mason, W. P. & Thurston, R. N.) 145–232 (Academic Press, 1984).
35. Noble, J. M. & Auvermann, H. J. The effects of large and small scale turbulence on sound propagation in the atmosphere. Army Research Laboratory, ARL-TR-565 (1995).
36. Berengier, M. C., Gauvreau, B., Blanc-Benon, P., Juve, D. & de Collongue, G. Outdoor sound propagation: a short review on analytical and numerical approaches. *Acta Acust. United Acust.* **89**, 980–991 (2003).
37. Ostashev, V. E. in *Sound-Flow Interactions* (eds Aurégan, Y., Pagneux, V., Pinton, J.-F. & Maurel, A.) 169–191 (Springer, 2002).
38. Garcia, R. F. et al. Finite-difference modeling of acoustic and gravity wave propagation in Mars atmosphere: application to infrasounds emitted by meteor impacts. *Space Sci. Rev.* **211**, 547–570 (2017).
39. Garcia, R. F., Lognonné, P. & Bonnin, X. Detecting atmospheric perturbations produced by Venus quakes. *Geophys. Res. Lett.* **32**, L16205 (2005).
40. Temel, O. et al. Large eddy simulations of the Martian convective boundary layer: towards developing a new planetary boundary layer scheme. *Atmos. Res.* **250**, 105381 (2021).
41. Spiga, A. et al. A study of daytime convective vortices and turbulence in the Martian planetary boundary layer based on half-a-year of InSight atmospheric measurements and large-eddy simulations. *J. Geophys. Res. Planets* **126**, e2020JE006511 (2021).
42. Colaïtis, A. et al. A thermal plume model for the Martian convective boundary layer. *J. Geophys. Res. Planets* **118**, 1468–1487 (2013).

the SuperCam team

R. C. Wiens[2], S. Maurice[1], T. Acosta-Maeda[22], C. Alvarez-Llamas[9], R. B. Anderson[23], S. M. Angel[10], D. M. Applin[24], G. Arana[25], M. Bassas-Portus[3], R. Beal[2], P. Beck[26], K. Benzerara[12], S. Bernard[12], P. Bernardi[7], T. Bertrand[7], O. Beyssac[12], T. Bosak[27], B. Bousquet[28], A. Brown[29], A. Cadu[3], P. Caïs[30], K. Castro[25], B. Chide[2], E. Clavé[28], S. M. Clegg[2], E. Cloutis[24], S. Connell[24], A. Cousin[1], A. Debus[31], E. Dehouck[32], D. Delapp[2], C. Donny[31], A. Dorresoundiram[7], G. Dromart[32], B. Dubois[33], C. Fabre[34], A. Fau[1], W. Fischer[35], O. Forni[1], T. Fouchet[7], R. Francis[11], J. Frydenvang[36], T. Gabriel[23], O. Gasnault[1], E. Gibbons[37], I. Gontijo[11], X. Jacob[6], J. R. Johnson[4], H. Kalucha[35], E. Kelly[22], E. W. Knutsen[8], G. Lacombe[8], N. L. Lanza[2], J. Laserna[9], J. Lasue[1], S. Le Mouélic[16], C. Legett IV[2], R. Leveille[37], E. Lewin[26], G. Lopez-Reyes[38], R. D. Lorenz[4], E. Lorigny[31], J. M. Madariaga[25], M. Madsen[36], S. Madsen[11], L. Mandon[7], N. Mangold[16], M. Mann[31], J.-A. Manrique[1,38], J. Martinez-Frias[39], L. E. Mayhew[40], T. McConnochie[41], S. M. McLennan[42], N. Melikechi[43], P.-Y. Meslin[1], F. Meunier[31], D. Mimoun[3], G. Montagnac[32], F. Montmessin[8], J. Moros[9], V. Mousset[31], N. Murdoch[3], T. Nelson[2], R. T. Newell[2], A. Ollila[2], Y. Parot[1], P. Pilleri[1], C. Pilorget[44,45], P. Pinet[1], G. Pont[31], F. Poulet[44], C. Quantin-Nataf[32], B. Quertier[30], W. Rapin[1], A. Reyes-Newell[2], S. Robinson[2], L. Rochas[31], C. Royer[7], F. Rull[38], V. Sautter[12], S. Schröder[20], S. Sharma[22], V. Shridar[11], A. Sournac[3], A. Stott[3], M. Toplis[1], I. Torre-Fdez[25], N. Turenne[24], T. Tzanetos[11], A. Udry[46], M. Veneranda[38], D. Venhaus[2], D. Vogt[20] & P. Willis[11]

[22]University of Hawai'i at Mānoa, Mānoa, HI, USA. [23]U.S. Geological Survey, Flagstaff, AZ, USA. [24]University of Winnipeg, Winnipeg, Canada. [25]University of the Basque Country UPV/EHU, Leioa, Bilbao, Spain. [26]Institut de Planétologie et Astrophysique de Grenoble, CNRS, Université Grenoble Alpes, Grenoble, France. [27]Department of Earth, Atmospheric and Planetary Sciences, Massachusetts Institute of Technology, Cambridge, MA, USA. [28]Centre Lasers Intenses et Applications, CNRS, CEA, Université de Bordeaux, Bordeaux, France. [29]Plancius Research, Severna Park, MD, USA. [30]Laboratoire d'Astrophysique de Bordeaux, CNRS, Université de Bordeaux, Bordeaux, France. [31]Centre National d'Études Spatiales, Toulouse, France. [32]Université de Lyon, UCBL, ENSL, UJM, CNRS, LGL-TPE, Villeurbanne, France. [33]Groupe d'Instrumentation Scientifique, Observatoire Midi-Pyrénées, Toulouse, France. [34]GeoRessources, CNRS, Université de Lorraine, Nancy, France. [35]California Institute of Technology, Pasadena, CA, USA. [36]University of Copenhagen, Copenhagen, Denmark. [37]McGill University, Montreal, Canada. [38]University of Valladolid, Valladolid, Spain. [39]Agencia Estatal Consejo Superior de Investigaciones Científicas, Madrid, Spain. [40]Department of Geological Sciences, University of Colorado Boulder, Boulder, CO, USA. [41]University of Maryland, College Park, MD, USA. [42]State University of New York, Stony Brook, NY, USA. [43]Department of Physics and Applied Physics, Kennedy College of Sciences, University of Massachusetts Lowell, Lowell, MA, USA. [44]Institut d'Astrophysique Spatiale, CNRS, Université Paris-Saclay, Orsay, France. [45]Institut Universitaire de France, Paris, France. [46]University of Nevada, Las Vegas, Las Vegas, NV, USA.

Environmental Effects on the Speed of Sound*

DENNIS A. BOHN

Rane Corporation, Mukilteo, WA 98275 USA

A detailed analysis of the environmental effects of temperature and humidity on the speed of sound is presented. An overview of the available literature reveals serious shortcomings for practical applications. New graphs, tables, and equations present the findings in a more useful manner for sound reinforcement “se. The results show that tight control of temperature and humidity must accompany the popular trend of splitting microseconds when time correcting sound systems. Failure to do so makes precise time correction a” exercise in futility.

0 INTRODUCTION

This paper presents, expands, and clarifies the environmental effects of temperature and humidity on the speed of sound. These effects increase the speed of sound and complicate the task of room equalization immensely—much more so than previously thought.

The dramatic effect of relative humidity on sound absorption appears as a separate section and helps explain many mysteries involving startling changes in room response from day to day. Even a modest change in relative humidity of only 10% can cause an additional 35 dB per 1000 ft (300 m) of absorption.

In one sense, nothing new appears in this paper. The major effects described and the equations presented all exist within published books on acoustics. Some from the *Journal of the Acoustical Society of America* are 45 years old. However, this does not reduce the importance of this paper. It is assumed that members of the Acoustical Society of America are familiar with this material. Unfortunately, very few people equalizing rooms for permanent sound systems belong to that society. This paper is for the members of the Audio Engineering Society who are in the trenches every day and need all the assistance they can get.

What *is* new is the table and graphic treatment of the material. Everything known regarding the effects of temperature and humidity on the speed of sound appears in this new form, as does the material on sound absorption. Experience shows tabulated and graphed data to he more useful than equations. Practical applications require concise look-up facts.

Before presenting the detailed analyses, a question should be answered: why bother?

This is not a facetious question. Many people realize that sound velocity depends upon temperature, barometric pressure, relative humidity, altitude, air composition, and so on. Only somewhere they learned that they may ignore these effects, that they are not significant. Well, 30 years ago the author may have agreed with you. Then we were just beginning to understand what room response meant, much less were we able to do anything about it. We then developed ways to view and alter room responses. Graphic equalizers and real-time analyzers opened up a whole new window of opportunity for improving playback audio.

Progress continued slowly until Richard Heyser gave us time-delay spectrometry (TDS). Then we experienced one of those step function jumps in our ability to view our acoustic environment. For the first time we could actually see what we had been dealing with all along.

Today we have a whole new army attacking room problems with a vengeance. Racks of equalizers and delay units arm these combatants as they wage war on all those response peaks and valleys. Each year they demand finer equalization tools and smaller delay increments with which to continue the fight. All this is fine. Only we must not forget mother nature. TDS-based test equipment allows us to see far more than is probably good for us. And there is a natural tendency to fix something if we can see it-without regard to relevancy.

The thesis of this paper is that tight control of temperature and relative humidity *must* accompany the use of very small time-delay increments to fix room response

* Presented at the 83rd Convention of the Audio Engineering Society, New York, 1987 October 16-19.

problems. Perhaps an example best illustrates the importance of tightly controlling the environment of sound systems.

0.1 An Example

For this example I will jump ahead and use data from the various graphs and tables presented. I hope this approach will encourage you to wade through the forthcoming material. As detailed as it must be, it is not terribly interesting. However, the results are.

This simple example does not even require diagrams. Consider a listening spot located such that the direct sound must travel 50 ft (15 m) to the listener. This same spot receives one reflected arrival that travels 140 ft (42 m), say 70 ft (21 m) to a sidewall and another 70 ft (21 m) back to the listener's ear. Ignore all other delayed arrivals. The reflected wave arrives with some sort of phase relationship to the direct wave. This relationship is a function of the distance traveled, the frequency involved, and the speed of sound.

Assume the room temperature was 20°C with 30% relative humidity when measurements where taken. Table 3 shows that the velocity of sound is 3.71% faster than standard velocity (1087.42 ft/s). Using a test tone of 10 kHz, calculate the following information:

Velocity of sound	1087.42 x 1.0371 = 1127.763 ft/s
Wavelength	$\frac{1127.763}{10\text{ kHz}} = 0.1127763$ ft
Number of cycles traveled for 50 ft	$\frac{50}{0.1127763} = 443.36$
Number of cycles traveled for 140 ft	$\frac{140}{0.1127763} = 1241.40$

For purposes of this example, the only thing of interest is the decimal fractions of a cycle. For all practical purposes the two waves are in phase (0.36 cycle verses 0.40 cycle), that is, the delayed and attenuated reflected wave arrives essentially in phase. So the two waves will add. A little equalization easily corrects this bump and the sound contractor is happy.

Until the environment changes. Assume the temperature rises to 30°C with 80% relative humidity. Consulting Table 3 shows that the velocity of sound now is 5.9% faster than standard. The casual observer mistakenly figures it is only a difference of 2.19%, so there is no problem. The casual observer is wrong.

Recalculation gives the following:

Velocity of sound	1087.42 X 1.059 = 1151.578 ft/s
Wavelength	$\frac{1151.578}{10\text{ kHz}} = 0.1151578$ ft
Number of cycles traveled for 50 ft	$\frac{50}{0.1151578} = 434.19$
Number of cycles traveled for 140 ft	$\frac{140}{0.1151578} = 1215.72$

Okay, the velocity of sound increased. This creates a longer wavelength. So traveling the same distances takes fewer cycles. Nothing too interesting yet. However, careful examination of the two decimal fractions of a cycle reveals that they are essentially *out of phase.* The difference between them is 0.53 cycle, or about 180°. Even to the casual observer this is not good. The applied equalization is now in the wrong direction.

This example illustrates the fallacy of thinking that you can ignore velocity changes since they affect direct and reflected waves equally. This simply is not true.

Complicating things further is the change in absorption due to the change in relative humidity. Table 6 and Fig. 6 show a drop of 39 dB per 1000 ft (300 m) due to the increased relative humidity (ignoring the temperature effects of 30°C). Since the example involves a distance of 140 ft, there is 5.46 dB less absorption. So not only does the signal arrive out of phase, but it is also about 5.5 dB bigger.

The point of all this is that even a small percentage change in the speed of sound can have disastrous effects on a sound system. Often overlooked is that *the small percentage change is for every cycle undergone by the wave.* It is a trap to think of the change as only a few percent and dismiss it. Think of the hundreds and thousands of cycles existing within any sound room. Each one has its wavelength altered by this percentage. If a 1% change affects hundreds of cycles, it alters the acoustics of the whole system. No wonder that all those hours spent equalizing are sometimes in vain.

0.2 Overview

Sec. 1 presents historical background information to put into perspective the number of years spent in investigating sound, its velocity, and the environmental factors affecting it. Temperature and humidity effects appear as Sec. 2. Following this, Sec. 3 outlines the effect of relative humidity on sound absorption, and finally, Sec. 4 gives a brief summary of the paper.

Much work lies ahead in understanding how to control environmental effects so that room equalization, once done, will remain satisfactory for prolonged periods. I hope this paper succeeds in outlining the necessary areas of study and in stimulating others to probe further.

1 HISTORICAL BACKGROUND [1]

Investigation into the nature of sound dates back to earliest recorded history. Indeed, ancient writings show that Aristotle (384-322 B.C.) observed two things regarding sound: first that the propagation of sound involved the motion of the air, and second that high notes travel faster than low notes. (Batting 0.500 is not too bad for the ancient leagues.)

Since in the transmission of sound air does not appear to move, it is not surprising that other philosophers later denied Aristotle's view. Denials continued until 1660 when Robert Boyle in England definitely concluded that air is one medium for acoustic transmission

The next question was, how fast does sound travel? As early as 1635, Pierre Gassendi, while in Paris, made measurements of the velocity of sound in air. His value

was 1473 Paris feet per second. (The Paris foot is approximately equivalent to 324.8 mm.) Later Marin Mersenne (1588 - 1648). a French natural philosopher often referred to as the "father of acoustics," corrected this to 1380 Paris feet per second, or about 450 m/s. Gassendi also demonstrated conclusively that velocity is independent of frequency, thus forever discrediting Aristotle's view.

In 1656 the Italian Borelli and his colleague Viviani made a very careful measurement and obtained 1077 Paris feet per second, or 350 m/s. It is clear that all these values suffer from a lack of reference to the temperature, humidity, and wind velocity conditions.

It was not until 1740 that the Italian Branconi showed definitely that the velocity of sound in air increases with temperature. This was two years after the French gave us our first good velocity figure.

The first measurement judged precise in the modern sense occurred under the direction of the Academy of Sciences of Paris in 1738, where cannon fire was used. When reduced to 0°C. the result was 332 m/s-a rather remarkable feat considering that careful repetitions during the rest of the eighteenth century and the first half of the nineteenth century gave results differing from this value by only a few meters per second. And 200 years later the best modern value [2] recorded was 331.45 ± 0.05 m/s in still, dry air under standard conditions of temperature and pressure (0°C and 760 mm of Hg pressure)--a scant 0.5-m/s difference from the French value.

Laplace was the first to show why temperature was important. He suggested that in all prior calculations errors occurred due to the assumption that the elastic motions of the air particles take place at constant temperature (isothermal law). In view of the rapidity of the motions, he reasoned that the gas molecules experience a small change in temperature. In 1816 he demonstrated that the compressions and rarefactions did not follow the isothermal law, but instead follow the adiabatic law in which the changes in temperature lead to a higher value of the elasticity. (Adiabatic refers to change in which there is no gain or loss of heat.)

Elasticity is the product of the pressure and the ratio of the two specific heats of the air. The ratio of the specific heats is symbolized by the lowercase Greek letter gamma. Laplace originally used results by LaRoche and Berard giving ??= 1.50. His results were off from the measured velocity, but not enough to discourage the theory. Later in his chapter on the velocity of sound in his *Mécanique Céleste* in 1825 he used the accurately measured value of ??= 1.35 by Clement and Desormes (1819). The revised calculations agreed very closely with experimental results. Some years later the revised value of ??= 1.40 led to complete agreement with the measured velocity.

The Laplace theory is so well established that it is now common practice to work backward to determine ??for various gases by precise measurements of the velocity of sound in the medium.

2 TEMPERATURE AND HUMIDITY EFFECTS ON THE SPEED OF SOUND

2.1 Introduction

This section presents the equations governing the temperature and humidity dependence of the speed of sound. All data are based on results published in the *CRC Handbook of Chemistry and Physics* [3] and in Hardy, Telefair, and Pielemeier's definitive paper [2].

2.2 General Equations

The theoretical expression for the speed of sound c in an ideal gas is

$$c = \sqrt{\frac{\gamma P}{p}} \tag{1}$$

where P is the ambient pressure, p the gas density, and ??the ratio of the specific heat of gas at constant pressure to that at constant volume.

The term ??is dependent upon the number of degrees of freedom of the gaseous molecule. The number of degrees of freedom depends upon the complexity of the molecule,

??= 1.67 for monatomic molecules
??= 1.40 for diatomic molecules
??= 1.33 for triatomic molecules.

Since air is composed primarily of diatomic molecules, the speed of sound in air is

$$c = \sqrt{\frac{1.4P}{p}} \tag{2}$$

The velocity of sound c in dry air has the following experimentally verified values:

$$c = 331.45 \pm 0.05 \text{ m/s} \tag{3}$$

or

$$c = 1087.42 \pm 0.16 \text{ ft/s} \tag{4}$$

for audio frequencies, at 0°C and 1 atm (760 mm Hg) with 0.03 mol-% of carbon dioxide.

2.3 Temperature Dependence

Substituting the equation of state of air of an ideal gas *(PV = RT)* and the definition of density p (mass per unit volume), Eq. (2) may be written as

$$c = \sqrt{\frac{1.4RT}{M}} \tag{5}$$

where R is the universal gas constant, T the absolute temperature, and M the mean molecular weight of the gas at sea level.

Eq. (5) reveals the temperature dependence and pressure independence of the speed of sound. An increase in pressure results in an equal increase in density.

Therefore there is no change in velocity due to a change in pressure. But this is true only if the temperature remains constant. Temperature changes cause density changes which do not affect pressure. Thus density is not a two-way street. Changes in pressure affect density but not vice versa. Humidity also affects density, causing changes in the velocity of sound. These effects are discussed in the next section.

Since R and M are constants, the speed of sound may be shown to have a first-order dependence on temperature as follows:

$$C_0 \sqrt{\frac{T}{273}} \tag{6}$$

where T is the temperature in kelvins and C_0 equals the reference speed of sound under defined conditions.

The speed of sound is seen to increase as the square root of the absolute temperature. Substituting centigrade conversion factors and the reference speed of sound gives

$$c := 331.45 \sqrt{1 + \frac{t}{273}} \tag{7}$$

or

$$c := 1087.42 \sqrt{1 + \frac{t}{273}} \tag{8}$$

where t is the temperature in degrees Celsius.

Graphs of Eqs. (7) and (8) are shown in Figs. 1 and 2, respectively. Table 1 tabulates results for Eqs. (7) and (8). A more useful presentation of these data is shown in Fig. 3, which graphs the percentage increase in the speed of sound due to temperature.

2.4 Humidity Dependence

All previous discussion assumed dry air. Attention turns now to the effects of moisture on the speed of sound. Moisture affects the density of air and hence, from Eq. (1). the speed of sound in air. Moist air is less dense than dry air (not particularly obvious), sop in Eq. (1) gets smaller. This causes an increase in the speed of sound. Moisture also causes the specific-heat ratio to decrease, which would cause the speed of sound to decrease. However, the decrease in density dominates, so the speed of sound increases with increasing moisture.

The literature is painfully lacking in practical specific treatments on the correlation between relative humidity and sound speed. Hardy et al. warn of the many inexact expressions existing in the textbooks, handbooks, and tables for the change in sound speed due to moisture. A rigorous analysis does exist in Pierce [4] and is used to develop a useful and accurate graph and table directly relating relative humidity to the percentage increase in the speed of sound.

Eq. (5) is exact for dry air. Two terms must be modified to include accurately the effects of moisture (water vapor) on the speed of sound. These are the specific-heat ratio (1.4 for dry air) and M, the average molecular weight of the different types of molecules in the air. Development of each of these terms follows. The terms R (universal gas constant) and T (absolute temperature) remain unchanged.

The specific-heat ratio ??can be expressed as an exact fraction by letting d equal the number of excited degrees of freedom for the air molecules. This gives

$$\gamma := \frac{d + 2}{d} \tag{9}$$

Since the composition of dry air is mostly two atom molecules, it is said to be a diatomic gas. Diatomic gases have 5 degrees of freedom, three translational and two rotational; thus d = 5 and ??= %, or 1.40, for dry air.

If h is defined to he equal to the fraction of molecules that are water, then the presence of water (with 6 degrees of freedom) causes the average number of degrees of freedom per molecule to increase to 5 + h. Eq. (9) can now be rewritten to include the effects of moisture for air **as**

$$\gamma_w := \frac{7 + h}{5 + h} \tag{10}$$

[It is noted that Eq. (10) is an alternative but equivalent

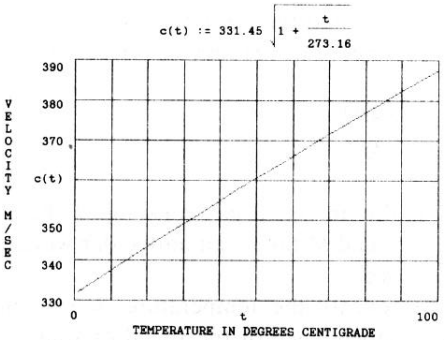

Fig. 1. Speed of Sound in m/s versus temperature.

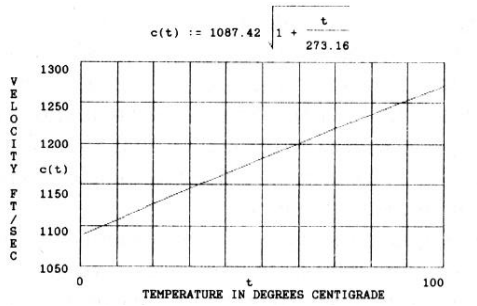

Fig. 2. Speed of sound in ft/s versus temperature.

expression to Humphreys's equation as used in thermodynamics.]

The average molecular weight of air decreases with added moisture. To see this, M is calculated first for dry air. Dry air composition is

78% nitrogen (molecular weight = 28)
21% oxygen (molecular weight = 32)
1% argon (molecular weight = 40)

for a total molecular weight equal to

$$M = (0.78)(28) + (0.21)(32) + (0.01)(40) = 29$$

The presence of water (with a molecular weight of 18) causes the total average molecular weight to decrease to 29 – (29 – 18) h, or

$$M_W := 29 - 11\,h \tag{11}$$

Eqs. (10) and (11) modify the two terms from Eq. (5) affected by the addition of water vapor to air. Both are a function of the introduced water molecule fraction h. Relative humidity RH (expressed as a percentage) is defined such that

$$h := \frac{0.01\mathrm{RH}\ e(t)}{p} \tag{12}$$

where p equals ambient pressure (1.013 X 10^5 Pa for 1 atm reference pressure) and $e(t)$ is the vapor pressure of water at temperature t. For temperature values in degrees Celsius, representative values of $e(t)$ are

e (5) = 872 Pa e (20) = 2338 Pa
e (10) = 1228 Pa e (30) = 4243 Pa
e (15) = 1705 Pa e (40) = 7376 Pa

To express the percentage increase in the speed of sound due to relative humidity all that remains is to take the ratio of the wet and dry speeds, subtract 1, and multiply by 100. Since both wet and dry speed terms involve the same constant terms (R and T), their ratio will cause these to cancel, leaving

$$\frac{c_w}{c_d} := \frac{\sqrt{\gamma_w/M_w}}{\sqrt{\gamma_d/M_d}} = \frac{\sqrt{\gamma_w/M_w}}{\sqrt{1.4/29}} = 4.5513\sqrt{\frac{\gamma_w}{M_w}}\,. \tag{13}$$

Subtracting 1 and multiplying by 100 yields

$$\text{increase in sound speed} = 455.13\sqrt{\frac{\gamma_w}{M_w}} - 100 \tag{14}$$

Eq. (14) is plotted in Fig. 4 as a function of relative humidity for six temperature values. Fig. 4 shows the percentage increase in sound speed due to relative humidity only; the temperature values are for accurately specifying the relative humidity. Table 2 gives calculated results for Eq. (14).

Table 1. Velocity of sound in dry air versus temperature.

Temperature (°C)	Temperature (°F)	Velocity (m/s)	Velocity (ft/s)
0	32.0	331.45	1087.42
1	33.8	332.06	1089.42
2	35.6	332.66	1091.39
3	37.4	333.27	1093.39
4	39.2	333.87	1095.36
5	41.0	334.47	1097.33
6	42.8	335.07	1099.30
7	44.6	335.67	1101.26
8	46.4	336.27	1103.23
9	48.2	336.87	1105.20
10	50.0	337.46	1107.14
11	51.8	338.06	1109.11
12	53.6	338.65	1111.04
13	55.4	339.25	1113.01
14	57.2	339.84	1114.95
15	59.0	340.43	1116.88
16	60.8	341.02	1118.82
17	62.6	341.61	1120.75
18	64.4	342.20	1122.69
19	66.2	342.78	1124.59
20	68.0	343.37	1126.53
21	69.8	343.96	1128.46
22	71.6	344.54	1130.37
23	73.4	345.12	1132.27
24	75.2	345.71	1134.20
25	77.0	346.29	1136.11
26	78.8	346.87	1138.01
27	80.6	347.45	1139.91
28	82.4	348.02	1141.78
29	84.2	348.60	1143.69
30	86.0	349.18	1145.59
31	87.8	349.75	1147.46
32	89.6	350.33	1149.36
33	91.4	350.90	1151.23
34	93.2	351.48	1153.13
35	95.0	352.05	1155.00
36	96.8	352.62	1156.87
37	98.6	353.19	1158.74
38	100.4	353.76	1160.61
39	102.2	354.32	1162.45
40	104.0	354.89	1164.32

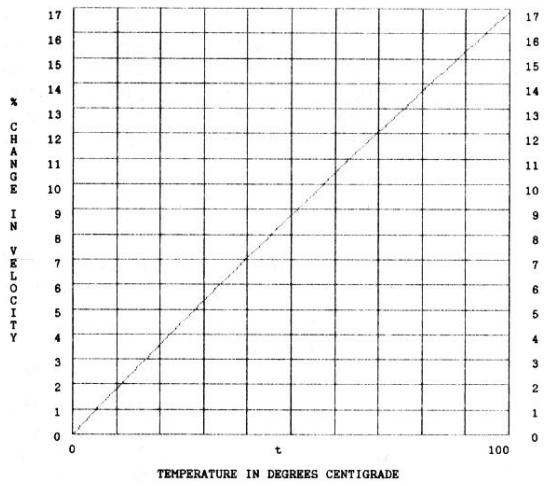

Fig. 3. Temperature versus percentage change in speed of sound (re 0°C) in dry air.

2.5 Combined Effects of Temperature and Relative Humidity

The results graphed in Figs. 3 and 4, and also tabulated in Tables 1 and 2, can be added together to show the combined effects of temperature and relative humidity on the speed of sound. Doing so produces Table 3. Here the total percentage increase in sound speed is tabulated for easy reference.

3 EFFECT OF RELATIVE HUMIDITY ON THE ABSORPTION OF SOUND IN AIR

3.1 Introduction

To a certain degree everything absorbs sound, especially air. Wet air absorbs sound better than dry air. This section presents the latest findings on the absorption of sound in air. The data are summarized in tables and graphs to highlight the effect of changing relative humidity on air absorption.

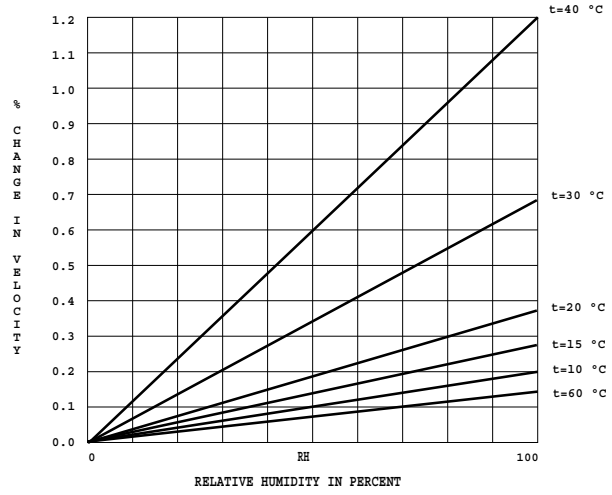

Fig. 4. Relative humidity versus percentage change in speed of sound as a function of temperature.

3.2 Air Absorption

Sound propagates through air as a wave in an elastic medium. Since air is not a perfectly elastic medium, this pulsating action causes several complex irreversible processes to occur. The wave action of air causes minute turbulence of the air molecules through which it passes. Each affected molecule robs the wave of some of its energy until eventually the wave dies completely. If this were not so, every sound generated would travel forever and we would live within a sonic shell of cacophony.

Absorption works with divergence. Divergence of sound causes a reduction in the sound intensity due to spreading of the wave throughout the medium. The sound pressure level will decrease 6 dB for each doubling of the distance, that is, it is inversely proportional to the square of the distance. This well-known fact occurs simultaneously with absorption. Absorption describes the energy-exchanging mechanism occurring during divergence. So not only is the wave spreading, it is also dying.

3.3 Air Absorption Mathematics

The strict confines of the ideal fluid-dynamic equations cannot explain the attenuation of sound. Theoretical predictions must include bulk viscosity, thermal conduction, and molecular relaxation for agreement with measured results. Conservation of mass, entropy for the gas, and molecular vibrations all enter into the thermodynamic equilibrium equations. To truly understand all the mechanisms of sound absorption in air, the interested reader must be ready to study molecular

Table 2. Percentage increase in speed of sound (re 0 °C) due to moisture in air only. Temperature effects not included except as they pertain to humidity.

Temperature	Relative humidity (%)									
(°C)	10	20	30	40	50	60	70	80	90	100
5	0.014	0.028	0.042	0.056	0.070	0.083	0.097	0.111	0.125	0.139
10	0.020	0.039	0.059	0.078	0.098	0.118	0.137	0.157	0.176	0.196
15	0.027	0.054	0.082	0.109	0.136	0.163	0.191	0.218	0.245	0.273
20	0.037	0.075	0.112	0.149	0.187	0.224	0.262	0.299	0.337	0.375
30	0.068	0.135	0.203	0.272	0.340	0.408	0.477	0.546	0.615	0.684
40	0.118	0.236	0.355	0.474	0.594	0.714	0.835	0.957	1.08	1.20

Table 3. Total percentage increase in speed of sound (re 0 °C) due to temperature and humidity combined.

Temperature	Relative humidity (%)					
(°C)	0	30	40	50	80	100
5	0.91	0.952	0.966	0.980	1.02	
10	1.81	1.87	1.89	1.91	1.97	2.01
15	2.71	2.79	2.82	2.85	2.93	2.98
20	3.60	3.71	3.75	3.79	3.90	3.98
30	5.35	5.55	5.62	5.69	5.90	6.03
40	7.07	7.43	7.54	7.66	8.03	8.27

kinetics, vibrational relaxation processes, and Navier-Stokes equations, and must know what a Laplacian is. Complete linear acoustic equations are not for the fainthearted. The mathematically courageous should refer to Pierce [4], where a painstakingly rigorous presentation is available.

Fortunately a simplified, yet accurate, alternate path exists. All of the above effects will combine into a term labeled total *attenuation coefficient* and designated by the letter m. This term is frequency, temperature, and humidity dependent [5]. For the case of a plane traveling wave, the following relationship holds [6]:

$$P = P_0 e^{-mx/2} \quad \textbf{(15)}$$

where P_0 is the pressure amplitude at distance $x = 0$, m is the total attenuation coefficient, and P is the pressure amplitude at distance x. Fig. 5 shows values of the total attenuation coefficient m versus relative humidity for air at 20°C and normal atmospheric pressure for frequencies between 2 and 12.5 kHz [7].

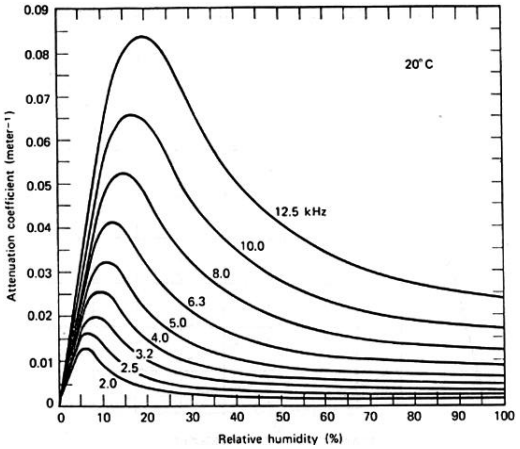

Fig. 5. Total attenuation coefficient m versus relative humidity for air at 20°C (68°F) as a function of frequency. From [7, p. 148].

Use Eq. (15) to obtain a direct expression relating loss in sound pressure level due to absorption. Dividing both sides by the reference pressure gives the ratio of the two pressures. Multiplying 20 times the log of both sides gives the sound pressure level (SPL) in decibels. Substituting a reference distance of 1000 ft (300 m) yields

$$\text{SPL loss in dB/1000 ft} = 20 \log e^{-500m} \quad \textbf{(16)}$$

where m derives from Fig. 5. Eq. (16) is accurate to within 1 or 2 dB per 1000 ft (300 m) compared with experimental results.

3.4 Experimental Results

An extensive compilation of sound absorption values versus relative humidity exists in Evans and Bass [8]. An abstract of this report appears in [3, pp. E-45 to E-48]. A summary of the most relevant frequencies for sound reinforcement is given in Tables 4 and 5.

Note that the first column gives the absorption figures for dry air. By subtracting out the dry air figures, new tables result which show only the increase in sound absorption due to relative humidity (Tables 6 and 7). Figs. 6 and 7 graph the information in Tables 6 and 7 to show the overall shape of the absorption curves. Comparison with Fig. 5 shows the expected similarity of curve shapes. (Figs. 6 and 7 are straight-line approximations to the continuous curve for the points given in Tables 6 and 7. Many more points would be necessary to show the smooth shape accurately.)

Table 4. Total sound absorption in dB/1000 ft (300 m) versus relative humidity as a function of frequency at 20°C (68°F).

Frequency (kHz)	Relative humidity (%)										
	0	10	**20**	**30**	40	50	**60**	**70**	80	90	100
2	**1.26**	**11.7**	**5.31**	**3.33**	**2.54**	**2.18**	**2.00**	1.92	1.89	1.89	1.92
4	**2.70**	**31.0**	19.0	11.9	**8.52**	**6.75**	**5.71**	**5.06**	**4.63**	**4.34**	**4.14**
6.3	**4.54**	**47.1**	**41.2**	**27.6**	**20.0**	**15.6**	**13.0**	11.2	9.98	9.10	**8.45**
10	8.01	61.6	79.7	**62.5**	**47.4**	**37.5**	**31.0**	**26.6**	**23.5**	**21.1**	19.4
12.5	10.9	**68.1**	**103**	89.7	70.9	**57.0**	**47.5**	**40.8**	35.9	**32.3**	29.5
16	15.9	**76.2**	**130**	129	**108**	89.6	**75.5**	**65.2**	**57.6**	**51.8**	**47.2**
20	**23.0**	**85.6**	**156**	**172**	155	**133**	**114**	99.4	**88.1**	79.4	**72.5**

Table 5. Total sound absorption in dB/km versus relative humidity as a function of frequency at 20°C (68°F).

Frequency (kHz)	Relative humidity (%)										
	0	10	**20**	**30**	**40**	50	60	**70**	80	90	100
2	**4.14**	**38.2**	**17.4**	**10.9**	**8.34**	**7.14**	**6.55**	**6.28**	**6.19**	**6.21**	**6.29**
4	**8.84**	**102**	**62.3**	**38.9**	**28.0**	**22.2**	**18.7**	**16.6**	**15.2**	**14.2**	**13.6**
6.3	**14.9**	**154**	**135**	**90.6**	**65.6**	**51.3**	**42.5**	**36.7**	**32.7**	**29.8**	**27.7**
10	**26.3**	**202**	**261**	**205**	**155**	**123**	**102**	**87.3**	**77.0**	**69.3**	**63.5**
12.5	**35.8**	**224**	**338**	**294**	**232**	**187**	**156**	**134**	**118**	**106**	**96.6**
16	**52.2**	**250**	**428**	**423**	**355**	**294**	**248**	**214**	**189**	**170**	**155**
20	**75.4**	**281**	**511**	**564**	**508**	**435**	**374**	**326**	**289**	**261**	**238**

3.5 Observations

Several important observations result from an examination of Figs. 6 and 7, the most obvious being that there is a critical range of relative humidity occurring between 10 and 40%. Within this range, the increase in sound absorption is greatest. This range also represents the most common relative humidity encountered. The steepness of the curves about this critical range with their rapid rate of change is very startling. Just a 10% change in relative humidity, from 10 to 20% for instance, at a frequency of 12.5 kHz results in an additional 35 dB per 1000 ft (300 m) of absorption. 1000 ft (300 m) may seem excessive, but that is an additional 3.5 dB per 100 ft (30 m), which could alter the acoustic response significantly. It could be the difference between two identical concerts, where one sparkles and has more brilliance than the other. Yet the same orchestra performed them in the same hall with the same exuberance and skill-only the weather was different.

This same increase in absorption will also cause a substantial decrease in reverberation time in auditoriums where surface absorption is low [9]. For very large halls with highly reflecting surfaces, air absorption at high frequencies can be the dominant phenomenon, and the change in absorption due to relative humidity can be the dominant factor determining whether a concert is spectacular or dull.

For frequencies below 2 kHz, sound absorption due to relative humidity is not significant and is ignored. For room sizes less than about 200,000 ft^3 (5400 m^3)

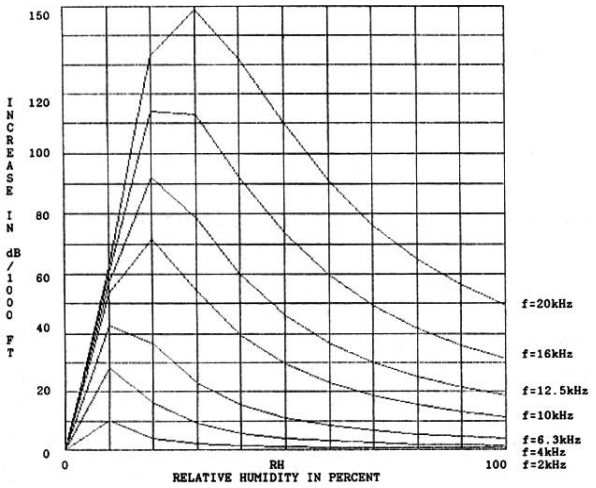

Fig. 6. Sound absorption increase in dB/l000 ft (300 m) versus relative humidity as a function of frequency at 20°C (68°F).

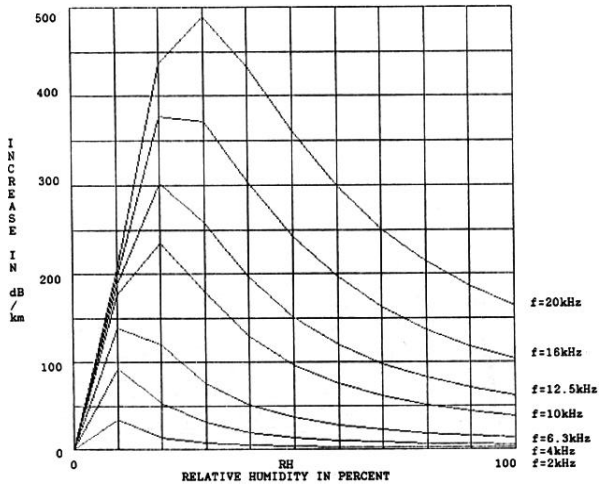

Fig. 7. Sound absorption increase in dB/km versus relative humidity as a function of frequency at 20°C (68°F).

Table 6. Increase in sound absorption in dB/l000 ft (300 m) due to relative humidity as a function of frequency at 20°C (68°F).

Frequency (kHz)	Relative humidity (%)										
	5	10	20	30	40	50	60	70	80	90	100
2	13.9	10.4	4.05	2.07	1.28	0.92	0.74	0.66	0.63	0.63	0.66
4	20.0	28.3	16.3	9.20	5.82	4.05	3.01	2.36	1.93	1.64	1.44
6.3	21.7	42.6	36.7	23.1	15.5	11.1	8.46	6.66	5.44	4.56	3.91
10	22.8	53.6	71.7	54.5	39.4	29.5	23.0	18.6	15.5	13.1	11.4
12.5	23.4	57.2	92.1	78.8	60.0	46.1	36.6	29.9	25.0	21.4	18.6
16	24.4	60.3	114	113	92.1	73.7	59.6	49.3	41.7	35.9	31.3
20	25.7	62.6	133	149	132	110	91.0	76.4	65.1	56.4	49.5

Table 7. Increase in sound absorption in dB/km due to relative humidity as a function of frequency at 20°C (68°F).

Frequency (kHz)	Relative humidity (%)										
	5	10	20	30	40	50	60	70	80	90	100
2	45.7	34.1	13.3	6.76	4.20	3.00	2.41	2.14	2.05	2.07	2.15
4	65.6	93.2	53.5	30.1	19.2	13.4	9.86	7.76	6.36	5.36	4.76
6.3	71.2	139	120	75.7	50.7	36.4	27.6	21.8	17.8	14.9	12.8
10	74.7	176	235	179	129	96.7	75.7	61.0	50.7	43.0	37.2
12.5	77.2	188	302	258	196	151	120	98.2	82.2	70.2	60.8
16	79.8	198	376	371	303	242	196	162	137	118	103
20	84.6	206	436	489	433	360	299	251	214	186	163

such as 100 by 100 by 20 ft (30 by 30 by 6 m)] sound absorption will not appreciably affect the *direct* sound. On the other hand, *reflected* sound covering great distances is affected, even in smaller rooms, that is, the reverberant sound field is more vulnerable than the direct sound field due to the distances involved.

4 SUMMARY

Environmental effects change the velocity and the absorption of sound in air. Even seemingly small percentage changes may cause serious listening problems in enclosed acoustic spaces. If room alignments down to tenths of an inch are to be meaningful, temperature and humidity should be controlled tightly.

Fractional changes in the wavelengths of frequencies traveling thousands of cycles can easily result in 180° phase reversal upon arrival. *No matter how small the change in the temperature, no matter how slight the humidity shift, the waves arrive shifted in phase and the resultant combination differs from the original.* It will not be the way it was when the room was equalized. Not only will the waves' phase be shifted, but for higher frequencies their magnitudes will be different due to the changes in absorption.

Much time is spent developing and using incremental time-delay devices to correct pictures shown by TDS instrumentation. An equal time spent in understanding and controlling the effects presented here is now required. The use of time-delay tools is valid, but remember, the implicit assumption being made is that the speed of sound does not change. Without rigid environmental controls this is a false assumption.

5 REFERENCES

[1] Based on R. B. Lindsay, "Historical Introduction," in J. W. S. Rayleigh, Ed., *The Theory of Sound* (Dover, New York, 1945).

[2] H. C. Hardy, D. Telefair, and W. H. Pielemeier, "The Velocity of Sound in Air," *J. Acoust. Soc. Am.*, vol. 13, pp. 226-233 (1942 Jan.).

[3] *CRC Handbook of Chemistry and Physics*, 67th ed. (CRC Press, Boca Raton, FL, 1986).

[4] A. D. Pierce, *Acoustics: An Introduction to Its Physical Principles and Applications* (McGraw-Hill, New York, 1981).

[5] L. B. Evans, H. E. Bass, and L. C. Sutherland, "Atmospheric Absorption of Sound: Theoretical Predications," *J. Acoust. Soc. Am.*, vol. 51, pp. 1565-1575 (1972).

[6] V. 0. Knudsen and C. M. Harris, *Acoustical Designing in Architecture* (Wiley, New York, 1950). p. 158.

[7] C. M. Harris, "Absorption of Sound in Air versus Humidity and Temperature," *J. Acoust. Soc. Am.*, vol. 40, pp. 148-159 (1966).

[8] L. B. Evans and H. E. Bass, "Tables of Absorption and Velocity of Sound in Still Air at 68°F (20°C)," AD-738576, National Technical Information Service, U.S. Department of Commerce, Springfield, VA 22151.

[9] F. W. White, *Our Acoustic Environment* (Wiley, New York, 1975). pp. 447-450.

THE AUTHOR

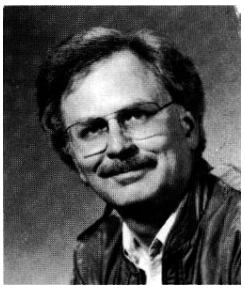

Dennis A. Bohn was born in San Fernando, California, in 1942. He received B.S.E.E. and M.S.E.E. degrees from the University of California at Berkeley in 1972 and 1974, respectively. Between undergraduate and graduate schools, he worked as a research and development engineer for the Hewlett-Packard Company developing thin-film high-speed oscillators. Upon completion of his M.S.E.E., he accepted a position with National Semiconductor Corporation as a linear application engineer specializing in audio. While at National Semiconductor, he created the *Audio Handbook*, acting as technical editor and contributing author. In 1976, he accepted the position of senior design engineer for Phase Linear Corporation, where he was involved in designing several consumer audio products. Promoted to engineering manager in 1978. he was responsible for developing the professional audio products division.

In 1982 Mr. Bohn's strong interest in professional audio products prompted him to leave Phase Linear and accept the position of vice president of engineering for Rane Corporation. In 1984, he became a principal of Rane Corporation and assumed the position of vice president in charge of research and development, where he now designs and develops advanced analog and digital products for the professional audio industry.

Mr. Bohn is a member of the AES, the IEEE, and Tau Beta Pi. For the past two years he has been listed in *Who's Who in the West.* Dozens of articles written by him have appeared in national and international magazines. He has also presented many papers at conventions of the Audio Engineering Society.